Hindawi
International Journal of Mathematics and Mathematical Sciences
Volume 2022, Article ID 5873432, 21 pages
https://doi.org/10.1155/2022/5873432

Research Article

A Mathematical Model for the Growth Dynamics of Demand in the Fashion Industry within the Era of the COVID-19 Pandemic

John Awuah Addor, Anthony Joe Turkson, and Douglas Yenwon Kparib

Department of Mathematics, Statistics and Actuarial Science, Takoradi Technical University, Sekondi-Takoradi, Ghana

Correspondence should be addressed to John Awuah Addor; john.addor@ttu.edu.gh

Received 1 December 2021; Revised 1 February 2022; Accepted 16 February 2022; Published 15 March 2022

Academic Editor: Theodore E. Simos

The outbreak of COVID-19 infection and its effects have not spared any economy on the globe. The fourth variant has just announced its appearance with its high death toll and impact on economic activities. The basic reproductive number (R_0), which measures the transmission potential of an infectious disease, is extremely important in the study of epidemiology. The main purpose of this study was to derive R_0 and assess the stability of the model around its equilibrium points. The motivation was to simulate the effect of COVID-19 on the demand for fashion products and how its application has impacted the COVID-19 pandemic. A five-compartment susceptible-infection-recovery-susceptible-based model was formulated in an integrated environment with application of fashion-based personal protective equipment (FPPEs) and government policy regulation, using ordinary differential equations. Solution techniques included a mix of qualitative analysis and simulations with data from various publications on COVID-19. The study revealed that the disease-free equilibrium was both locally and globally asymptotically stable (LAS and GAS) for $R_0 \leq 1$, while the disease-endemic equilibrium was both LAS and GAS for $R_0 \geq 1$. As the demand for FPPEs increases, R_0 decreases, and vice versa. The sensitivity analysis indicated that R_0 was very sensitive to the rate of application of FPPEs. This confirms the significance of high demand for FPPEs in reducing the transmission of COVID-19 infection. Again, the pandemic has had both positive and negative impacts on the demand for fashion products; however, the negative impact outweighed the positive impact. Another discovery was that government policy stringency was significant in increasing demand for FPPEs. The sensitivity analyses suggested prioritization of FPPEs application together with all recommended PPEs. We recommend inter alia that FPPEs be used together with other nonpharmaceutical interventions. Operators in the fashion industry must be dynamic in adjusting to the new trends of taste for fashion products. Finally, governments should maintain high policy stringency.

1. Introduction

The economic effect of the novel corona virus disease has been felt by almost every country in the world. Local communities have been drastically affected, resulting in an increase in crime, domestic violence, prices, and low business productivity, and there were also significant reduction in income, a rise in unemployment, and disruptions in transportation services and manufacturing industries [1–4]. The outbreak of the disease (COVID-19), which triggered the novel coronavirus-infected pneumonia (NCIP), has affected the lives of 252 million people globally, with over 5.2 million succumbing to death. The disease, which originated from Wuhan city in China, rapidly spread to other countries. The disease is caused by a severe acute respiratory syndrome, corona virus (SARS-CoV-2) [5–9]. The outbreak of the disease was declared as a pandemic on March 11, 2020, by WHO after it had hit over 200 countries of the world [10]. Ghana recorded its first case on March 12, 2020, and as of now, 131,000 lives have been affected with about 1200 people succumbing to death. The COVID-19 pandemic, by virtue of its fast-spreading trend, has since its emergence changed the normal ways of doing things across the globe [11, 12]. In the absence of an orthodox cure for COVID-19, the application of nonpharmaceutical interventions (NPIs) has become very popular. Interventions are as follows: social distancing;

country-wide lockdowns; contact tracing; quarantine of persons suspected to be exposed to the virus; COVID-19 awareness programs; isolation and hospitalization of confirmed cases; application of face shield and nose-masks; washing of hands with soap and/or application of alcohol-based hand sanitizer; restrictions of social events; close down of schools, entertainment centers, inter alia as reported by [13–17] in [18–21]. While these measures were instituted to reduce overcrowding or the possibility of interaction between the susceptible group and infected individuals (especially the asymptomatic), which constituted the salient source of transmission of infection, efforts were also made to boost human immune systems. Currently, vaccines have been produced, and worldwide vaccination is smoothly underway. COVID-19 statistics from the world dataset as referenced in [22] show that, as of November 30, 2021, approximately 55.8% of the world population have been vaccinated with at least one dose of the COVID-19 vaccine. In terms of total dosage of vaccines administered, 7.72 billion doses have been administered across the globe. On a daily basis, 27.67 million doses are administered. Woefully, only 5% of people in low-income countries, especially Africa, have received at least one dose. In Ghana, between May 31, 2021, and November 30, 2021, 842,770 (2.7%) people have been fully vaccinated against the disease, while 1.69 million (5.3%) people have received partial vaccination against COVID-19 [22].

The application of NPIs as measures to contain the spread and transmission of COVID-19 infection has ubiquitously affected public health, political, and economic life [21, 23]. According to [1], the enforcement of NPIs in market places was exemplified by improving hygienic conditions via disinfection of all markets, closure of markets to enforce social distancing among traders, and imposition of lockdown to decongest densely populated markets. Administrative enforcement of COVID-19 preventive measures or NPIs measures affected the production and distribution of goods and services. Some goods such as petroleum products were in excess due to restrictions on international as well as local movements, while others such as food and clothing were possibly in shortage culminating in price hikes. The shortfall in the production or supply of certain goods and services could be explained by the government's enforcement of preventive measures aimed at decongesting densely populated centers, which served as the industrial or manufacturing hub. These centers were the epicenters for the transmission of COVID-19 infection. Individual personal preventive initiatives due to fear of being infected might have contributed to the closure of private manufacturing companies; finally, some manufacturers capitalized on the COVID-19 pandemic to redirect resources from the manufacturing business to the production of personal protective/preventive equipment popularly known as PPEs.

Among the industries that were operationally affected in the pandemic era was the fashion industry. It is eminent to classify the effect of this pandemic on the growth of the fashion industry into both positive and negative effects. The positive effect is represented by the growth of the fashion industry due to the increase in the demand for fashion-typified PPEs (which shall be referred to as FPPEs), while the negative effect is proxied by the decline in the growth of the fashion industry owing to the decline in the demand for non-FPPEs and other normal fashion products. The net effect will then be the sum of the two effects. Invariably, one effect will outweigh the other. The positive effect could be influenced by government policy regulation, which enforced the use of FPPEs such as nose masks, face-shields/masks, hand gloves, among other things. This effect shall be labelled as safety or precautionary measures. On the other hand, the negative effects emanated from interaction-based government policy regulation, which shall also be referred to as restrictive policies. In the literature, the effective role of NPIs in curtailing the rapid rate of transmission of COVID-19 has extensively been confirmed. However, to the best of our knowledge, the impact of NPIs on the demand for goods and services has received little or no attention. This confirms the originality of the paper. The main purpose of this study was to derive the basic reproduction number (R_0) and assess the stability of the model around its equilibrium points. The motivation was to simulate the effect of the COVID-19 pandemic on the growth of the demand for fashion products, and the role of application of FPPEs in curtailing the spread of COVID-19 transmission. The strategic objectives of the study were fourfold: to develop SIRS model for COVID-19 in a heterogeneous environment with demand for (or application of) FPPEs and government policy regulation; compute both the effective and basic reproductive numbers; analyze the stability of the models; and perform numerical simulations.

The study added to the existing theory by highlighting certain salient integrated government and individual interventions that promoted and sustained the growth of the fashion industry in the era of the pandemic. It also provided insight into the effects of safety-based and interaction-based restrictions on the demand for fashion products. The role of government policy stringency on increasing demand for FPPEs was also expanded. The introduction of FPPEs also provided an opportunity to simulate the effects of fashion-based PPEs on the transmission of COVID-19 infection. Integrating demand for fashion products into the SIRS model was also new as far as available literature was concerned. All the above elements introduced new perspectives, which were significant contribution to theory on the COVID-19 pandemic.

1.1. Theoretical Framework. A lot of mathematical models have been developed in several research endeavors to analyze the spread of COVID-19 infection. For instance, in [15], a mathematical modelling of COVID-19 epidemic awareness program was proposed to assess the dynamics of COVID-19 transmission in Nigeria. Integrated in the model was an awareness program and diverse hospitalization techniques for both mild and severe cases with a view to evaluating the impact of public knowledge on the dynamics of the transmission of COVID-19 infection. After fitting the model to a cumulated number of confirmed cases in Nigeria, the likelihood of the epidemic to increasing the event of

ineffective handling of awareness programs was established. The findings further suggested that awareness programs and timely hospitalization constituted effective control, mitigation, or eradication tools for COVID-19 in Nigeria. In [24], quarantine and hospitalization were integrated in the formulation and analysis of a deterministic model to predict the transmission risk of COVID-19 infection and its possible consequences on public health interventions. An extension of this model was considered by [25]. In this extended version, two subcompartmentalization sections, hospitalized/isolated individuals and those in intensive care units of the infectious compartment, were explored to investigate the role of nonpharmaceutical interventions in flattening the spread of COVID-19 infection. [5] also used a simple susceptible-exposed-infectious-recovery (SEIR) based model to predict the spread of COVID-19 both within and beyond China. The estimated R_0 showed an epidemic doubling in 6.4 days, which characterized the exponential growth nature of the spread of the COVID-19 infection. In [14], another deterministic model was designed by integrating the impact of myriad quarantine interventions in a dynamic study of COVID-19 infection transmission to assess the effectiveness of some salient epidemiological correlates as control measures. Their findings revealed that the rates of contact and recovery of asymptomatically infected persons constituted major parameters for effective control of transfer of COVID-19 infection in Wuhan city of China, thereby confirming the significance of quarantine and hospitalization in combating the pandemic. [26] formulated a conceptual model for the transmission of COVID-19 infection in China. The model incorporated individual behavioral reactions and governmental action. After computing the possible future trends and reporting ratio of the virus, the possible correlate of the outbreak was captured, and an extensive explanation was advanced to enhance understanding of the trend of the outbreak. A new deterministic model was developed in [27] for the spread of COVID-19 infection to analyze the effectiveness of quarantine and isolation in controlling the epidemic in Pakistan. Qualitative analysis of the model was performed in line with the existence, uniqueness, boundedness, and equilibria of the model. The results indicated the persistence of the epidemic in Pakistan as evidenced from the R_0 value of 1.3. They, therefore, recommended, based on the real data for incremental active cases, that the quarantine period be increased to reduce the pending cases of transmission of COVID-19 infection. A mechanistic model was developed to evaluate the effectiveness of the application of face masks to the susceptible population in mitigating the spread of COVID-19 infection [28]. The application of face masks by the public was revealed to be of much relevance in combating the burden of the pandemic. The mass benefit was likely to be maximized if face masks were applied in addition to nonpharmaceutical interventions and greater massive acceptance and compliance.

In New York, the impact of the lockdown on air pollution was investigated. In general, the results revealed that there was a significant decline in air pollution as a result of lockdown; this finding has the potential of providing a critical environmental implication for researchers and academicians [29]. [30] considered the stringency index (government measures/policies in response to the COVID-19 outbreak) for each cross section in the panel data. The index indicators included school closures, workplace closures, and travel bans. Quantile regressions revealed significant negative estimated impacts of stringency policy on COVID-19 total cases.

Studies on various aspects of COVID-19 pandemic revealed that the pandemic had resulted in distressing job conditions for frontline medical workers in terms of increased anxiety symptoms; sustained psychological distress; emotional exhaustion; clinically significant depression; perceived risk of infection; excessive workload; reduced availability of personal protective equipment; inadequate professional support; perceived risk of contracting COVID-19 and transmitting the virus to the loved ones, which might lead to developing stress-related psychiatric disorders; burnout syndrome; elevated anxiety symptoms; and clinically significant depression among medical personnel; development of psychiatric symptoms; significant depression; extreme anxiety; and burnout syndrome due to intense workload and increased responsibilities; constant exposure to mainstream journalism and social media coverage of COVID-19 pandemic reporting. Other studies looked at the main sources of false or misleading information about COVID-19 and relationship between virus anxiety, emotional contagion, and responsible media [31–36].

2. Materials and Methods

In this section, we developed a simple mathematical model that exemplified the growth dynamics of the fashion industry in this era of COVID-19 pandemic. The model was a five-state nonlinear system of ordinary differential equations (ODEs), where the states were represented by susceptible population S, COVID-19 infected population (I), recovered population (R), application of PPEs, which is used synonymously with the demand for PPEs (A), and government policy regulation (G). This constituted the SIRS model with emphasis on the effect of COVID-19 infection on the growth of the fashion industry on the one hand, and the role of the fashion industry in mitigating the accelerated rate of spread of this SARS-CoV-2 disease. Practically, the effect of COVID-19 infection on the growth of the fashion industry represented just an aspect of the complete economic effect of the SARS-CoV-2. It is eminent to classify the effect of this pandemic on the growth of the fashion industry into both positive and negative effects, where the positive effect was represented by the growth of the fashion industry due to the increase in the demand for FPPEs, while the negative effect was proxied by the decline in the growth of the fashion industry owing to the decline in the demand for non-FPPEs and other normal fashion products. The net effect will then be determined by which category of effect outweighs the other. Thus, in our model, the state A assumes the role of a predator since the trend of the disease had revealed that the demand for fashion-based PPEs (FPPEs) and their subsequent applications thrived on the existence of COVID-19 infection and its eventual increase. As COVID-19 increases,

the demand for FPPEs and its subsequent application by the susceptible group increases. The implication is that the application of FPPEs in public places will decrease as COVID-19 infection declines and will eventually decay to zero in the absence of COVID-19 infection. State I, on the other hand, assumes the role of the prey in that COVID-19 infection thrives in the absence of FPPEs application, but its curve flattens with the application of FPPEs. The underpinning assumptions of this model are as follows:

(i) The demand for FPPEs depends only on the existence of COVID-19; this means that FPPEs are applied because of the COVID-19 pandemic

(ii) Increase in demand for FPPEs implies an increase in the application of the same; this ensures that once FPPEs are purchased, they will be applied

(iii) COVID-19 decreases at a rate proportional to the rate of FPPE application; the implication is that as the application of FPPEs increases at a given rate, COVID-19 also decreases by the same rate

(iv) Recovered individuals gain partial immunity after which they lose it and regain susceptibility; this also implies that infected individuals who recover from COVID-19 infection can be reinfected

The variables and parameters are defined in Tables 1 and 2.

The SIRS model is diagrammatically represented in Figure 1.

The model is represented by a continuous time nonlinear system of ODEs specified as

$$\left.\begin{aligned}
\frac{\mathrm{d}S}{\mathrm{d}t} &= \pi_s N + \mu_3 R - \sigma_1 S - \frac{\mu_1 \omega (1-\pi_1) SI}{N},\\
\frac{\mathrm{d}I}{\mathrm{d}t} &= \frac{\mu_1 \omega (1-\pi_1)}{N} SI - (\sigma_1 + \sigma_2 + \mu_2) I,\\
\frac{\mathrm{d}R}{\mathrm{d}t} &= \mu_2 I - (\sigma_1 + \mu_3) R,\\
\frac{\mathrm{d}A}{\mathrm{d}t} &= K + \gamma G + kA - \pi_2 A,\\
\frac{\mathrm{d}G}{\mathrm{d}t} &= (I - I_{trh})\beta - \mu_4 G = 0,
\end{aligned}\right\}. \quad (1)$$

The initial conditions that accompany the governing equations of equation (1) are given as

$$\{S(0) = S_0, I(0) = I_0, R_0 = R(0), A(0) = A_0, G(0) = G_0\} \geq 0. \quad (2)$$

We note critically in equation (1) that the susceptible population (S) increases as more members are recruited into S through births (π_s). The recovery rate μ_3, which represents the rate at which members of the recovery state lose their partial or short-term immunity, also serves as another source of inflow to S. Similarly, the rate of FPPE application π_1 is a source of increment to the state S since the transmission is a function of the behavior pattern (or adherence) of the susceptible population to government regulations and laid-down (safety or precautionary) COVID-19 protocols [37]. This means that the rate of transfer of infection into the state I is reduced at a rate π_1 due to the application of FPPEs. However, S decreases as its members interact with the COVID-19 infectious population (I) at a transmission rate of infection μ_1. A further decremental factor to the population S is the natural death rate (σ_1), which constitutes a source of decrement to every other state in the system represented by equation (1). The infectious state faces competing risks from the recovery state (R) at a recovery rate μ_2. Other sources of outflows to the state I are π_1 (the rate of FPPEs application or demand, which has already been explained as the rate of reduction in transfer of infection from state S into the state I), and the death rates σ_1 and σ_2 which are the proxy, respectively, of the natural death rate and the death rate due to COVID-19 infection. Conversely, the infectious population obtains increment from S at a transmission rate μ_1 due to interactions with S. The expression I/N in equation (1) is called the force of infection. Explaining further, the recovery state R increases as the infected population recovers at a rate μ_2 but decreases through the natural death rate σ_1 and transition to the state S at a rate μ_3 of loss of immunity. In this model, the birth rate constitutes the only source of recruitment rate into the population; immigration is ignored to allow concentration on community or horizontal transmission of the COVID-19 infection. This assumption can be justified by the strict protocols that are observed at various entry points of all countries worldwide to reduce the incidence of vertical transmission of COVID-19 infection in all countries. Horizontal transmission increases due to community interactions among members of susceptible and infected populations, which serves as a determining factor for the accelerated rate of COVID-19 infection at a rate μ_1. The demand for FPPEs (A) in the wake of COVID-19 infection is assumed, in this paper, to be partly constant K. It also obtains inflows at FPPEs application-based policy with intensity γ, and integrated personal interventions in respect of intensity of FPPEs application k. On the aspect of competing risks, the state A decreases in proportion to itself at a rate π_2 of movement-based (or interaction-based) policy restrictions. These forms of restrictions are imposed to restrict movement and possible interactions among the susceptible community through social gathering or any form of social events or activities that promote interpersonal

Table 1: Definition of model variables.

Variable	Definition
S	The susceptible population
I	The infectious population
R	The recovered population
A	The demand for or application of FPPEs
G	Government policy regulation

Table 2: Definition model parameters.

Parameter	Definition
π_s	Recruitment rate into the population.
μ_1	The transmission rate of infection.
μ_2	The rate at which the infected population recovers.
μ_3	The rate at which recovered individuals lose their partial immunity.
π_1	The rate of FPPEs application.
π_2	The rate of decrease in FPPEs application due to social restriction policy.
σ_1	The natural death rates.
σ_2	Death rate of transmission of COVID-19 infection.
Υ	The intensity of policy enforcement on the application of FPPEs.
ω	The rate of contact between susceptible and infectious individuals.
β	Policy stringency index implemented at an infection threshold Itrh.
μ_4	The force of policy relaxation.
κ	The intensity of personal level intervention in respect of FPPEs application.
K	Independent demand for fashion product.
I_{trh}	A transmission threshold above which policy stringency is applied or enforced.

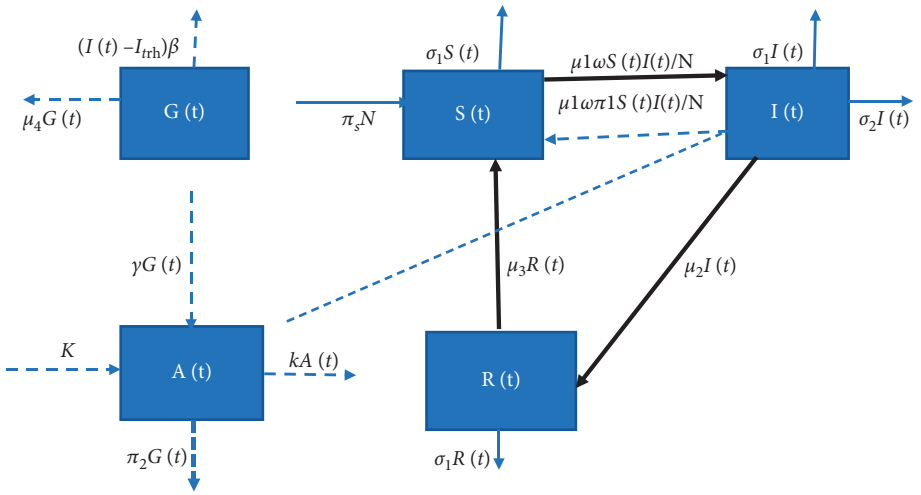

Figure 1: Depiction of the model. The gaps between the compartments indicate a flow only in the direction of the arrows. For instance, the flow from $G(t)$ to $A(t)$ is an inflow to $A(t)$ but not an outflow to $G(t)$. Due to the application of FPPEs, the transmission of infection from state S to state I will reduce at a rate π_1. The states (S) I, (R) A, and G are continuous functions of time.

interactions. It may also take the form of total or partial lockdown. As the transmission of infection increases to a given threshold I_{trh}, government policy regulation (G) will be enforced with a stringency index β. After some time, policy efforts will decline (due to negligence and other negative attitude on the side of the government machinery) with a relaxation force μ_4 proportional to itself. It is assumed that government policy regulation will be applied in two dimensions; the first is a movement-based restriction policy (lockdown, prohibition of all forms of social activities or gathering, inter alia). The second relates to policy enforcement on precautionary or safety measures such as PPEs application in general, of which FPPEs is a constituent, social distancing, among others.

2.1. Positivity of the Solution. Let us define a two-dimensional time-continuous dynamical system of the form

$$\left.\begin{aligned}
\frac{dP_f}{dt} &= f(S, I, R, A, G),\\
\frac{dI}{dt} &= g(S, I, R, A, G),\\
\frac{dR}{dt} &= h(S, I, R, A, G),\\
\frac{dA}{dt} &= \omega(S, I, R, A, G),\\
\frac{dG}{dt} &= \varphi(S, I, R, A, G),
\end{aligned}\right\} \tag{3}$$

where $f\colon R^5 \longrightarrow R$, $g\colon R^5 \longrightarrow R$, $h\colon R^5 \longrightarrow R$, $\varphi\colon R^5 \longrightarrow R$ and $\omega\colon R^5 \longrightarrow R$ are continuous differentiable functions and

R is the set of real numbers. A solution $g: R^5 \longrightarrow R$ of equation (2) is uniquely obtained by the initial conditions $(S_0, I_0, R_0, A_0, G_0) \in R^5$ and satisfies $\{N = (S, I, R, A, G) \longrightarrow R^5: S_0 > 0, I_0 > 0, R_0 > 0, A_0 > 0, G_0 > 0\}$.

The task under this section is to demonstrate that the unique solution (S, I, R, A, G) of equation (1) is positive.

Theorem 1. *Let* $\Phi = \{(S, I, R, A, G) \longrightarrow R^5: S_{0A} > 0, I_0 > 0, R_0 > 0, A_0 > 0, E_0 > 0\}$. *Then, the solution* (P_f, I, R, A, G) *is positive for* $t \geq 0$.

Proof. From the system (1), we have

$$\left.\begin{aligned} \frac{dS}{dt} &\geq -(\mu_1 \omega I + \sigma_1)S, \\ \frac{dI}{dt} &\geq -(\mu_1 + \sigma_1 + \sigma_2 + \mu_1 \omega S)I, \\ \frac{dR}{dt} &\geq -(\sigma_1 + \mu_3)R, \\ \frac{dA}{dt} &\geq -\pi_2 A, \\ \frac{dG}{dt} &\geq -\mu_4 G, \end{aligned}\right\} \tag{4}$$

Treating the equations of equation (3) separately, we perform separation of variables and subsequently, integrated to obtain

$$\begin{aligned} S(t) &\geq K\exp[-(\mu_1 \omega I + \sigma_1)t], \\ I(t) &\geq K\exp[-(\mu_1 + \sigma_1 + \sigma_2 + \mu_1 \omega S)t], \\ R(t) &\geq K\exp(\sigma_1 + \mu_3)t, \\ A(t) &\geq K\exp(-\pi_2 t), \\ G(t) &\geq K\exp(-\mu_4 t). \end{aligned} \tag{5}$$

Applying the initial conditions reduces the above equations to

$$\begin{aligned} S(t) &\geq S_0\exp[-(\mu_1 \omega I + \sigma_1)t], \\ I(t) &\geq I_0\exp[-(\mu_1 + \sigma_1 + \sigma_2 + \mu_1 \omega S)t], \\ R(t) &\geq R_0\exp[-(\sigma_1 + \mu_3)t], \\ A(t) &\geq A_0\exp(-\pi_2 t), \\ G(t) &\geq G_0\exp(-\mu_4 t). \end{aligned} \tag{6}$$

Since $(\mu_1 \omega I + \sigma_1) > 0$, $(\mu_1 + \sigma_1 + \sigma_2 + \mu_1 \omega S) \geq 0$, $(\sigma_1 + \mu_3) > 0$, $\pi_2 > 0$ and $\mu_4 > 0$, it is obvious that the above inequalities are positive thereby establishing the proof of Theorem 1.

2.2. Invariant Region

Theorem 2. *The closed region* ϕ *is positively invariant, which contains or absorbs all possible unique solution* (S, I, R, A, G) *of equation (1).*

Proof.

Given the total population $N = S + I + R + A + G$, there exists a variant region ϕ which absorbs all the solution of equation (1). Intuitively, all the solutions (S, I, R, A, E) of equation (1) are positive and bounded within ϕ. Let $N = N_1 + N_2 + N_3$, where $N_1 = S + I + R$, $N_2 = A$ and $N_3 = G$.

From the first three equations of the system (1), we obtain

$$\frac{dN_1}{dt} \geq \pi_s N - \sigma_1 N_1. \tag{7}$$

Integrating after separation of variables, we have

$$\begin{aligned} &\ln|\pi_s N - \sigma_1 N_1| \leq K - \sigma_1 t, \\ &\Rightarrow \pi_s N - \sigma_1 N_1 \leq K\exp(-\sigma_1 t). \end{aligned} \tag{8}$$

Applying the initial conditions yields

$$\begin{aligned} &K \geq \pi_s N_0 - \sigma_1 N_{01}, \\ &\Rightarrow \pi_s N - \sigma_1 N_1 \leq (\pi_s N_0 - \sigma_1 N_{01})\exp(-\sigma_1 t). \end{aligned} \tag{9}$$

Now, the infimum of the population N is obtained by

$$\begin{aligned} &\lim_{t \longrightarrow \infty} N_1 \leq \lim_{t \longrightarrow \infty}\left[\frac{\pi_s N - (\pi_s - \sigma_1 N_{01})\exp(-\sigma_1 t)}{\sigma_1}\right], \\ &\Rightarrow \lim_{t \longrightarrow \infty} N_1 \leq \frac{\pi_s N}{\sigma_1}. \end{aligned} \tag{10}$$

Also, from the fourth equations, given that $k_2 = \pi_2 - k$, we obtain

$$\frac{dN_2}{dt} \geq K - k_2 N_2. \tag{11}$$

By integrating and applying the initial value conditions, we have

$$\begin{aligned} &K - k_2 N_2 \geq (K - k_2 N_{02})exp(-k_2 t), \\ &\Rightarrow \lim_{t \longrightarrow \infty} N_2 \leq \frac{K}{k_2}. \end{aligned} \tag{12}$$

Similarly, we obtain the following inequality from the fifth equation:

$$\begin{aligned} &\frac{dN_3}{dt} \leq \beta I - \mu_4 N_3, \\ &\Rightarrow \lim_{t \longrightarrow \infty} N_3 \leq \frac{\beta I}{\mu_4}. \end{aligned} \tag{13}$$

Hence, from equations (4), (5), and (6), the population N satisfies $0 \le N \le \{\pi_s N/\sigma_1\} \bigcup \{K/k_2\} \bigcup \{\beta I/\mu_4\}$, which characterizes the invariant region:

$$\Phi = \left\{(S, I, R, A, G) \in R^5 : S + +I + R \le \frac{\pi_s N}{\sigma_1},\ A \le \frac{K}{k_2},\ G \le \frac{\beta I}{\mu_4}\right\}. \tag{14}$$

It is clear from the above proof that all the solutions (S, I, R, A, G) are bounded within the positive invariant region Φ. This completes the proof of Theorem 2.

Theorem 3. *A system of the form equation (1) is said to be well-posed if its solution (S, I, R, A, G) is positive and bounded within a positive invariant region.*

Proof.

Following the proof of Theorems 1 and 2, it can be established that equation (1) is biologically, socially, economically, and mathematically well-posed.

2.3. COVID-19 Infection Free Equilibrium. In this section, we compute and subject the COVID-19 infection-free equilibrium (COVIFE) to stability analysis. The key target of policy efforts by the World Health Organization (WHO), National Health Systems, governments, and all other stakeholders is to eradicate COVID-19.

COVIFE analysis, therefore, constitutes an essential attempt to discover the crucial correlates of this COVID-19 pandemic.

To compute COVIFE, we set $S = I = R = A = G = 0$ with the following condition. Let COVIFE be represented by $E^0 = (S^0, I^0, R^0, A^0, G^0)$. Then, by equating each of the governing equations of equation (1) to zero as represented by equations (7) to (11).

$$\begin{aligned}
\pi_s N + \mu_3 R - \sigma_1 S^0 - \frac{\mu_1 \omega (1 - \pi_1)}{N} S^0 I^0 &= 0,\\
\frac{\mu_1 \omega (1 - \pi_1)}{N} S^0 I^0 - (\sigma_1 + \sigma_2 + \mu_2) I^0 &= 0,\\
\mu_2 I^0 - (\sigma_1 + \mu_3) R^0 &= 0,\\
K + \gamma G^0 + k A^0 - \pi_2 A^0 &= 0,\\
\left(I^0 - I_{trh}\right)\beta - \mu_4 G^0 &= 0.
\end{aligned} \tag{15}$$

At the disease-free equilibrium, $I = 0$, $R = 0, G = 0$; and by considering the region Φ, we solve to obtain

$$E^0 = \left(\frac{\pi_s N}{\sigma_1}, 0, 0, \frac{K}{\pi_2 - k}, 0\right). \tag{16}$$

Definition 1. Let $(S^*, I^*, R^*, A^*, G^*)$ be an equilibrium point of a map $H(u, v, w, x, y, z) = \{f(u, v, w, x, y, z),\ g(u, v, w, x, y, z), h\ (u, v, w, x, y, z), \varphi(u, v, w, x, y, z), \omega(u, v,\ w, x, y, z)\}$, where f, g, h, ω, and φ are functions that are continuous and differentiable at the equilibrium point $(S^*, I^*, R^*, A^*, G^*)$. A linearize form of equation (2) about $(S^*, I^*, R^*, A^*, G^*)$ can be expressed as

$$H\left(S^*, I^*, R^*, A^*, G^*\right) = H(X) = J_{S^*, I^*, R^*, A^*, E^*} X. \tag{17}$$

where $X = (S^*, I^*, R^*, A^*, G^*)^T$ and $J_{S^*, I^*, R^*, A^*, G^*}$ represents the Jacobian matrix about the equilibrium point $(S^*, I^*, R^*, A^*, G^*)$.

Now, from equation (1), we have

$$J_{S,I,R,A,G} = \begin{bmatrix}
-\left[\sigma_1 + \dfrac{\mu_1 \omega (1 - \pi_1)}{N} I\right] & -\dfrac{\mu_1 \omega (1 - \pi_1)}{N} S & \mu_3 & 0 & 0\\
\dfrac{\mu_1 \omega (1 - \pi_1)}{N} I & \dfrac{\mu_1 \omega (1 - \pi_1)}{N} S - (\sigma_1 + \sigma_2 + \mu_2) & 0 & 0 & 0\\
0 & \mu_2 & -(\sigma_1 + \mu_3) & 0 & 0\\
0 & 0 & 0 & k - \pi_2 & \gamma\\
0 & \beta & 0 & 0 & -\mu_4
\end{bmatrix}. \tag{18}$$

Evaluating the Jacobian matrix at the COVIFE $E_1^0 = (\pi_s/\sigma_1, 0, 0, K/\pi_2 - k, 0)$, where $S = N$, we obtain

$$J_{S^*,I^*,R^*,A^*,G^*} = J_{\frac{\pi_s N}{\sigma_1},0,0,\frac{K}{\pi_2-k},0} = \begin{bmatrix} -\sigma_1 & -\mu_1\omega(1-\pi_1) & \mu_3 & 0 & 0 \\ 0 & \mu_1\omega(1-\pi_1)-(\sigma_1+\sigma_2+\mu_2) & 0 & 0 & 0 \\ 0 & \mu_2 & -(\sigma_1+\mu_3) & 0 & 0 \\ 0 & 0 & 0 & k-\pi_2 & 0 \\ 0 & \beta & 0 & 0 & -\mu_4 \end{bmatrix}. \tag{19}$$

From $J_{\pi_s N/\sigma_1,0,0,K/\pi_2-k,0}$, we compute the characteristics polynomial $P_5(\lambda)$ defined by

$$P_5(\lambda) = \left| J_{\frac{\pi_s N}{\sigma_1},0,0,\frac{K}{\pi_2-k},0} - \lambda I_5 \right| = 0, \tag{20}$$

where I_5 is the (5×5) identity matrix.

2.4. Stability Analysis of COVIFE

Theorem 4. *Let $(S^*, I^*, R^*, A^*, G^*)$ be the equilibrium points of equation (3) and $J_{S_A^*,S_A^*,I^*,R^*}X$ be the corresponding linearized system about the equilibrium points. Then, equation (3) is locally asymptotically stable if all the eigenvalues $\lambda_n (n = 1, 2, 3, 4)$ of the Jacobian matrix J_{S^*,I^*,R^*,A^*,G^*} satisfy $\lambda_n < 0$. Otherwise, it is not locally asymptotically stable.*

Proof

Computing the eigenvalues of the characteristic polynomial $P_5(\lambda)$ above, we obtain

$$\begin{aligned} \lambda_1 &= -\sigma_1, \\ \lambda_2 &= \mu_1\omega(1-\gamma) - (\sigma_1+\sigma_2+\mu_2+\pi_1), \\ \lambda_3 &= -(\mu_3+\sigma_1), \\ \lambda_4 &= k-\pi_2, \\ \lambda_5 &= -\mu_4, \end{aligned} \tag{21}$$

where

$$P_5(\lambda) = (\lambda+\mu_4)(\lambda+\pi_2)AB = 0.$$

$$\begin{aligned} A &= \left(\lambda^2 + \lambda\mu_3 + 2\lambda\sigma_1 + \mu_3\sigma_1 + \sigma_1^2\right). \\ B &= \left(-\lambda - \mu_2 - \pi_1 + \frac{\mu_1\omega(1-\gamma)\pi_s}{\sigma_1} - \sigma_1 - \sigma 2\right). \end{aligned} \tag{22}$$

Following from Theorem 4, since four of the eigen values $(\lambda_1, \lambda_3, \lambda_5) < 0$, the requirement for local asymptotic stability is partly satisfied. Additional conditions to satisfy the local asymptotic stability criterion are given by

$$\mu_1\omega(1-\gamma) < (\sigma_1+\sigma_2+\mu_2+\pi_1), \tag{23}$$

and

$$k < \pi_2. \tag{24}$$

The effective reproductive number R^* can be derived as

$$R^* = \frac{\mu_1\omega(1-\pi_1)}{\sigma_1+\sigma_2+\mu_2} + \frac{k}{\pi_2}. \tag{25}$$

The effective reproductive number represents the partial contributions of the natural birth rate, death rate due to infection, the recovery rate, and movement-based restriction rate to COVID-19. In the absence of movement-based restrictions, $\pi_2 = 0$, and the basic reproductive number R_0 becomes

$$R_0 = \frac{\mu_1\omega(1-\pi_1)}{\sigma_1+\sigma_2+\mu_2}. \tag{26}$$

In the context of this paper, basic reproductive number refers to the average number of secondary infections that can be caused by a single case of the COVID-19 infection within the susceptible population during the entire period of infectivity. For an infectious disease such as COVID-19, equation (1) is stable if the basic reproductive number R_0 is defined such that $R_0 < 1$. The system is unstable if $R_0 > 1$.

Thus, we have the basic reproductive number $R_0 = k_1 < 1$.where $\pi_s = \sigma_1$ and

$$k_1 = \frac{\mu_1\omega(1-\pi_1)}{\sigma_1+\sigma_2+\mu_2}. \tag{27}$$

The conditions for local asymptotic stability are met; hence, equation (1) is locally asymptotically stable.

A critical observation reveals that the contact and transmission rates (ω and μ_1) relate positively to the basic reproductive number R_0, whereas the rate of FPPEs application (π_1), the death rate of transmission (σ_2), the recovery rate (μ_2), and the natural death rate (σ_1) are inverse determinants of R_0. The role of application of FPPEs and the COVID-19 recovery rate in decreasing the basic reproductive number is, therefore, made very obvious given the inverse relationship between them and the average number of secondary infections that one single infection may generate in the entire infective period as defined by R_0.

To perform the global stability analysis, we applied the following method developed by [37]. We defined

$$\frac{dX_1}{dt} = F(X_1, X_2),$$
$$\frac{dX_2}{dt} = H(X_1, X_2), \tag{28}$$
$$H(X_1, 0) = 0,$$

where $X_1 = (S_0, R_0, A_0, G_0)$ and $X_2 = (I_0)$; $X_1 \in R^4$ can be described as a vector that represents a heterogeneous state of noninfectious group, and $X_2 \in R$ is a vector that represents the state of the infectious group. $E^* = (X_1^0, 0)$ represents the COVIFE of the system (1), where $X_1^0 = (N^0, 0)$ and $N^0 = N_1^0 + X_2^0 + X_3^0$. In addition, let us define

$$A = J_{X_2} H(X_1, X_2), \tag{29}$$

where $J_{X_2} H(X_1, X_2)$ is the Jacobian of $H(X_1, X_2)$ with respect to X_2; it is an M-matrix whose off-diagonal elements are nonnegative. Following the theorem in [37], the following theorem for global asymptotic stability (GAS) holds.

Theorem 5. *The COVIFE point E^* for equation (1) is GAS if, in addition to $R_0 \le 1$, we have*

P. $dX_1/dt = F(X_1, 0)$, E^0 is GAS.

Q. $H(X_1, X_2) = AX_2 - \overline{H}(X_1, X_2), \overline{H}(X_1, X_2) \ge 0$ for $(X_1, X_2) \in \phi$ where $\in\in\phi$ at the point where the model makes biological sense.

Proof

Given that $X_1 = (S_0, R_0, A_0, G_0)$ and $X_2 = (I_0)$, we have

$$F(X_1, 0) = \begin{cases} \pi_s N^0 - \sigma_1 S^0, \\ -\sigma_1 R^0, \\ K + kA^0 - \pi_2 A^0, \\ -\mu_4 G^0. \end{cases} \tag{30}$$

Solving $F(X_1, 0)$ as a linear differential equation, we have

$$\begin{cases} S^0(t) = \dfrac{\pi_s N^0}{\sigma_1} - \dfrac{\pi_s N^0(0)}{\sigma_1} \exp(-\sigma_1 t) + S^0(0) \exp(-\sigma_1 t), \\ R^0(t) = R^0(0) \exp(-\sigma_1 t), \\ A_0(t) = \dfrac{K}{k_2} - \dfrac{K}{k_2} \exp(-k_2 t) + A^0(0) \exp(-k_2 t), \\ G_0(t) = G^0(0) \exp(-\mu_4 t), \end{cases} \tag{31}$$

where $k_2 = \pi_2 - k$ and $k < \pi_2$.

It is obvious from the above that $S^0(t) + R^0(t) + A^0(t) + G^0(t) \longrightarrow N^0(t)$ as $t \longrightarrow \infty$, independent of the values of $S^0(t)$, $R^0(t)$, $A^0(t)$ and $G^0(t)$. Thus, P of Theorem 5 is established and E^0 is GAS.

Moreover, we have

$$H(X_1, X_2) = \begin{bmatrix} \dfrac{\mu_1 \omega (1 - \pi_1)}{N} S_0 I_0 - (\sigma_1 + \sigma_2 + \mu_2) I_0 \\ 0 \\ 0 \\ 0 \end{bmatrix},$$

$$A = J_{X_1} H(X_1, X_2) \text{where } X_2 = (I_0, 0, 0, 0),$$

$$AX_2 = \begin{bmatrix} \dfrac{\mu_1 \omega (1 - \pi_1)}{N} S_0 - (\sigma_1 + \sigma_2 + \mu_2) & 0 & 0 & 0 \\ 0 & 0 & 0 & 0 \\ 0 & 0 & 0 & 0 \\ 0 & 0 & 0 & 0 \end{bmatrix} \begin{bmatrix} I_0 \\ 0 \\ 0 \\ 0 \end{bmatrix},$$

$$AX_2 = \begin{bmatrix} \dfrac{\mu_1 \omega (1 - \pi_1)}{N} S_0 I_0 - (\sigma_1 + \sigma_2 + \mu_2) I_0 \\ 0 \\ 0 \\ 0 \end{bmatrix}$$

$$= H(X_1, X_2),$$

$$\Rightarrow \overline{H}(X_1, X_2) = \begin{bmatrix} 0 \\ 0 \end{bmatrix}. \tag{32}$$

This is an obvious satisfaction of the inequality $\overline{H}(X_1, X_2) \ge 0$.

Since P and Q are satisfied, it follows from the above theorem that the disease or infection-free equilibrium of equation (1) is GAS.

2.5. COVID-19 Infection Endemic Equilibrium. In this section, we compute the pandemic equilibrium of equation (6). In this steady state solution, the disease does not die out of the population. We denote the COVID-19 infection pandemic equilibrium (COVIPE) by $E^* = (S^*, I, {}^*R^*A, {}^*G^*)$. The endemic equilibrium is computed by setting

$$\begin{aligned}\frac{dS}{dt} &= \frac{dI}{dt}\\ &= \frac{dR}{dt}\\ &= \frac{dA}{dt}\\ &= \frac{dG}{dt}\\ &= 0\end{aligned} \tag{33}$$

Equation (1) now reduces to

$$\begin{aligned}\pi_s N + \mu_3 R - \sigma_1 S^* - \frac{\mu_1\omega(1-\pi_1)}{N}S^*I^* &= 0,\\ \frac{\mu_1\omega(1-\gamma)}{N}S^*I^* - (\sigma_1+\sigma_2+\mu_2)I^* &= 0,\\ \mu_2 I^* - (\sigma_1+\mu_3)R^* &= 0,\\ K + \gamma G^* + kA^* - \pi_2 A^* &= 0,\\ (I^* - I_{trh})\beta - \mu_4 G^* &= 0.\end{aligned} \tag{34}$$

Solving equations (7) to (11) simultaneously, we obtain the endemic equilibrium $E^* = (S^*, I^*, R^*, A^*, G^*)$, where

$$\begin{aligned}S^* &= \frac{K_0}{K_1}N,\\ I^* &= \frac{N(\sigma_1+\mu_3)[\pi_s K_1 - k_0\sigma_1]}{K_1[(K_0+\mu_3)\sigma_1 + \mu_3\sigma_2]},\\ R^* &= \frac{\mu_2 N[\pi_s K_1 - k_0\sigma_1]}{K_1[(K_0+\mu_3)\sigma_1 + \mu_3\sigma_2]},\\ G^* &= \frac{(I^* - I_{trh})\beta}{\mu_4},\\ A^* &= \frac{K+\gamma G^*}{\pi_2 - k},\\ K_0 &= \sigma_1+\sigma_2+\mu_2,\\ K_1 &= \mu_1\omega(1-\pi_1).\end{aligned} \tag{35}$$

Analyze the stability of the COVIPE, we compute the Jacobian J_{S^*,I^*,R^*,A^*,G^*} around the pandemic equilibrium $E^* = (S^*, I^*, R^*, A^*, G^*)$. We obtain

$$J_{S^{\∗},I^*,R^*,A^*,G^*} = \begin{bmatrix} -\left[\sigma_1 + \frac{\mu_1\omega(1-\pi_1)}{N}I^*\right] & -\frac{\mu_1\omega(1-\pi_1)}{N}S^* & \mu_3 & 0 & 0\\ \frac{\mu_1\omega(1-\pi_1)}{N}I^* & \frac{\mu_1\omega(1-\pi_1)}{N}S^* - (\sigma_1+\sigma_2+\mu_2) & 0 & 0 & 0\\ 0 & \mu_2 & -(\sigma_1+\mu_3) & 0 & 0\\ 0 & 0 & 0 & k-\pi_2 & \gamma\\ 0 & \beta & 0 & 0 & -\mu_4 \end{bmatrix}. \tag{36}$$

Solving for the eigenvalues, we obtain two eigenvalues as follows:

$$\begin{aligned}&\lambda_4 = k - \pi_2, \Rightarrow \lambda_4 < 0 \text{ if } k < \pi_2,\\ &\lambda_5 = -\mu_4 < 0.\end{aligned} \tag{37}$$

The characteristic polynomial $P_3^*(\lambda)$ that characterizes the remaining three eigenvalues is given by

$$P_3^*(\lambda) = \lambda^3 + A_2\lambda^2 + A_1\lambda + A_0, \tag{38}$$

where

$$
\begin{aligned}
A_2 &= K_0 + \frac{K_1 I^* - K_1 S^*}{N} + \mu_3 + 2\sigma_1,\\
\mathrm{A}_1 &= -\frac{\mu_3 K_1 S^*}{N} - \frac{2\sigma_1 K_1 S^*}{N} + \mu_3\sigma_1\\
&\quad + \sigma_1^2 + \frac{(K_0 + \mu_3 + \sigma_1)}{N} K_1 I^*\\
&\quad + (\mu_3 + 2\sigma_1)K_0,\\
\mathrm{A}_0 &= \frac{\sigma_1(\mu_3 + \sigma_1)(\mathrm{K}_0 N - K_1 S^*)}{N}\\
&\quad + \frac{[(\mu_3 + \sigma_1)K_0 - \mu_2\mu_3]K_1 I^*}{N}.
\end{aligned}
\tag{39}
$$

Theorem 6. *(The Routh–Hurwitz's stability criterion).*

Let J_{S^*,I^*,R^*,A^*,G^*} be the Jacobian matrix of equation (1) about the endemic equilibrium $E^* = (S^*, I^*, R^*, A^*, E^*)$ with a characteristic polynomial $P_5(\lambda) = \lambda^5 + A_4\lambda^4 + A_3\lambda^3 + A_2\lambda^2 + A_1\lambda + A_0$. Let any two arbitrary eigenvalues $\lambda_1, \lambda_2 < 0$, and then the characteristic polynomial $P_5(\lambda)$ reduces to a third-order polynomial, $P_3(\lambda) = \lambda^3 + A_2\lambda^2 + A_1\lambda + A_0$. Equation (1) is both locally and globally asymptotically stable around $(S^*, I^*, R^*, A^*, G^*)$ if, in addition to the fact that $\lambda_1, \lambda_2 < 0$, we have $A_2 > 0, A_0 > 0$ and $A_2A_1 > A_0$.

Proof.

If $A_2 \geq 0$, it is required to show that

$$
\begin{aligned}
&\Rightarrow K_0 + \frac{K_1 I^* - K_1 S^*}{N} + \mu_3 + 2\sigma_1 > 0,\\
&\Rightarrow \frac{K_1 I^* - K_1 S^*}{N} \geq 0.
\end{aligned}
\tag{40}
$$

By substituting the values of I^* and S^*, we obtain

$$
\begin{aligned}
&\frac{(\sigma_1 + \mu_3)K_0}{[(K_0 + \mu_3)\sigma_1 + \mu_3\sigma_2]}[\pi_s R_0 - \sigma_1] - K_0 > 0,\\
&\Rightarrow \frac{(\sigma_1 + \mu_3)K_0\pi_s}{[(K_0 + \mu_3)\sigma_1 + \mu_3\sigma_2]}\left(R_0 - \frac{\sigma_1}{\pi_s}\right) - K_0 > 0.
\end{aligned}
\tag{41}
$$

By assuming a steady state equilibrium condition, the birth rate and natural death rate are equal, so we have

$$
\frac{(\sigma_1 + \mu_3)K_0\pi_s}{[(K_0 + \mu_3)\sigma_1 + \mu_3\sigma_2]}(R_0 - 1) - K_0 > 0. \tag{42}
$$

Clearly, the above inequality holds if $R_0 > 1$. Thus, $A_2 > 0$ if $R_0 > 1$.

Also, to show that $A_0 > 0$, we simplify as follows:

$$
\begin{aligned}
\mathrm{A}_0 &= \frac{\sigma_1(\mu_3 + \sigma_1)(\mathrm{K}_0 N - K_1 S^*)}{N} + \frac{[(\mu_3 + \sigma_1)K_0 - \mu_2\mu_3]K_1 I^*}{N},\\
&\Rightarrow \mathrm{A}_0 = \frac{[(\mu_3 + \sigma_1)K_0 - \mu_2\mu_3]K_1 I^*}{N},\\
&\Rightarrow \mathrm{A}_0 = \frac{K_1 I^*}{N}[(\mu_3 + \sigma_1)\mathrm{K}_0 - \mu_2\mu_3],\\
&\Rightarrow \mathrm{A}_0 = \frac{(\sigma_1 + \mu_3)[(\mu_3 + \sigma_1)\mathrm{K}_0 - \mu_2\mu_3]K_0\pi_s}{[(K_0 + \mu_3)\sigma_1 + \mu_3\sigma_2]}[R_0 - 1].
\end{aligned}
\tag{43}
$$

A careful evaluation of the value for A_0 indicates that for $\mathrm{A}_0 > 0$, $R_0 \geq 1$.

Finally, we show that $A_2A_1 > A_0$. If the value of I^* is substituted into A_1, we have

$$
\begin{aligned}
\mathrm{A}_1 &= -\frac{\mu_3 K_1 S^*}{N} - \frac{2\sigma_1 K_1 S^*}{N} + \mu_3\sigma_1 + \sigma_1^2\\
&\quad + \frac{(K_0 + \mu_3 + \sigma_1)}{N} K_1 I^* + (\mu_3 + 2\sigma_1)K_0,\\
\Rightarrow \mathrm{A}_1 &= \mu_3\sigma_1 + \sigma_1^2 + \frac{(K_0 + \mu_3 + \sigma_1)}{N} K_1 I^*,\\
\mathrm{A}_1 &= \frac{(\sigma_1 + \mu_3)(K_0 + \mu_3 + \sigma_1)K_0\pi_s}{[(K_0 + \mu_3)\sigma_1 + \mu_3\sigma_2]}[R_0 - 1] + \mu_3\sigma_1 + \sigma_1^2.
\end{aligned}
\tag{44}
$$

For $R_0 = 1$, we have

$$
\mathrm{A}_2\mathrm{A}_1 = (\mu_3\sigma_1 + \sigma_1^2)(\mu_3 + 2\sigma_1) > 0 = A_0. \tag{45}
$$

Hence, for $R_0 \geq 1$, $\mathrm{A}_2\mathrm{A}_1 > A_0$. It is important to note that $R_0 = 1$ does not satisfy $A_0 > 0$. Thus,

$$
\mathrm{A}_2 > 0,\ \mathrm{A}_0 > 0 \text{ and } \mathrm{A}_2\mathrm{A}_1 > 0 \text{ given that } R_0 > 1. \tag{46}
$$

The above accomplishes the proof of Theorem 6. Thus, the system represented by equation (1) assumes both local and global stability status at a disease-endemic equilibrium if the basic reproductive number $R_0 \geq 1$. The system is unstable at a disease endemic equilibrium if $R_0 \leq 1$ and infection will then persist without dying out.

2.6. Numerical Simulations

2.6.1. Parameter Estimates. Table 3 presents the values for all parameters used and their sources. Some of the parameters were adjusted from previous publications. In cases where a given parameter belongs to a number of categories, an aggregated form is considered by computing a common average for such a parameter.

The initial values were taken from the updated number of cases, recoveries, and deaths with reference to October 24, 2021 (WorldOmeter). These are recorded in Table 4.

By applying the initial values and parameters, we obtain a time series plot for *S*, *I*, *R*, *A* and *G*, as Figure 2 illustrates.

Table 3: Parameter estimates and sources.

Parameter	Value/range (units)	Source
N	30, 985, 230	[38, 39]
πs	0.00008 (day-1)	Computed based on [39]
$\mu 1$	0.168 (day-1)	Community transmission rate [15, 38, 40]
$\mu 2$	0.09 [(1/7 + 1/12 + 1/31.5)/3] (day-1)	Computed based on [31]
$\mu 3$	1/60 (day-1)	Partial immunity rate [38]
$\mu 4$	10 (%)	Assumed for simulations
$\pi 1$	0.67 (day-1)	Adjusted based on [41]
$\pi 2$	0.2 (day-1)	Assumed for simulations
$\sigma 1$	0.00001 day-1	Computed and truncated based on [39]
$\sigma 2$	0.02 day-1	[38]
γ	0.12 (%)	Assumed for simulations
ω	0.97 [0–1] day-1	Set based on [38]
β	45 [40–50] (%)	Set based on [42]
k	0.15 [0–1]	Set based on [38]
K	0.3	Assumed
Itrh	1000	Set based on equilibrium value of I

Table 4: Initial values for S, I, R, A, and G.

Variable	Initial values	Source
S	30728886	Computed using N
I	129, 805	WorldOmeter
R	126, 539	WorldOmeter
A	16978	Assumed
G	2000	Assumed

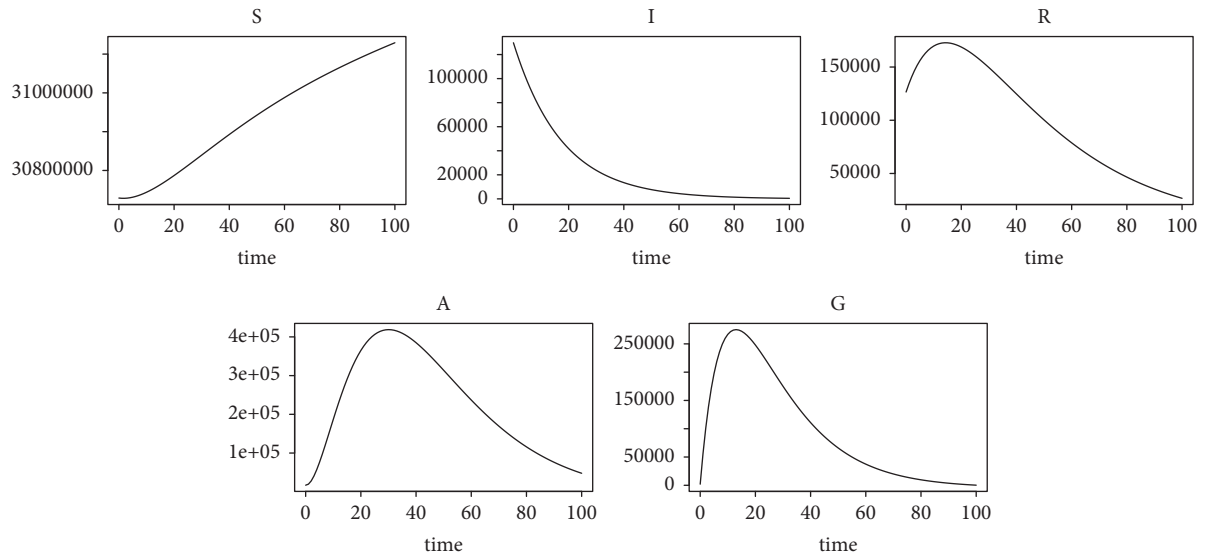

Figure 2: Time series of the susceptible class (S), infectious class (I), recovered class (R), demand for FPPES (A), and government policy regulation (G).

The susceptible population keeps on increasing over the entire simulation period. The infected population is on a continuous downward trend after its peak, and the recovered class rose to a peak but started declining thereafter on a daily basis. The demand for fashion products depicts a bell or dome shape; it rises, attains its peak, and falls thereafter, and government policy regulation follows the same trend.

The relationships between I, R, A and G are depicted in Figure 3.

The relationship among the infected, recovered, demand for products of the fashion industry and government policy regulation has been depicted in Figure 3. When all period infection was at its peak, government policy and demand for products of the fashion industry

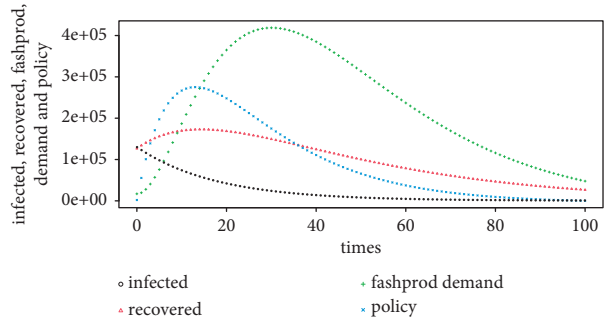

Figure 3: Time series plot of infected, recovered, demand for fashion products and policy.

were high. However, as infection declines, government policy regulation and demand for fashion products follow suite. Recovery increases at a rate higher at the peak of infection, at which time government policy regulation and demand for fashion products were on the upward trend. Infection falls at a faster rate between period 0 and 40, but the rate of decline in government policy regulation and demand for fashion products was faster. With the slower pace of decline in the rate of infection (between periods 40 and 100), government policy regulation and demand for products of the fashion industry decline faster. The rate of recovery also declines faster but eventually equates that of infection at the end of the period.

2.7. Sensitivity Analysis. In this section, we performed a sensitivity analysis of the model's parameters that determines the basic reproductive number R_0. In general, sensitivity analysis refers to a measure of the degree of responsiveness of the basic reproductive number to a change in the model parameters. Determining the sensitivity of R_0 relative to small perturbations in the model's parameters constitutes a test of the robustness of the model. Sensitivity analysis provides a useful guide for policy formulation in respect of the parameters of the model. Policy makers are able to determine which parameters to control in an epidemiology outbreak to inform effective control. Sensitivity analysis, therefore, serves as a useful guide to prioritize policy interventions in the event of a pandemic such as the outbreak of COVID-19 infection [2, 15]. Mathematically, if the R_0 depends on the parameters θ_i, then the sensitivity of R_0 relative to θ_i is defined by

$$\theta_i^{R_0} = \frac{\partial R_0}{\partial \theta_i} \times \frac{\theta_i}{R_0}. \tag{47}$$

Results of the sensitivity analysis suggested that the most sensitive parameter was π_1. Any percentage intervention in respect of π_1 results to a more than proportionate reduction in the spread of the disease since π_1 is negatively related to the infection transmission rate μ_1. Government should therefore prioritize policy towards the application of FPPEs together with other PPEs.

3. Results and Discussion

The simulation presents a trend that represents the reality of COVID-19 in relation to time, susceptibility, infection, recovery, demand for or application of FPPEs, and government policy regulation and its effectiveness. The results are discussed below.

3.1. The Basic Reproductive Number ($\mathbf{R}_0$). As has already been confirmed in any typical epidemiology study and all other studies in respect of the COVID-19 pandemic, the basic reproductive number is positively determined by the transmission rate of infection. In this study, a variation in the transmission rate of infection by 20% induces approximately 20% increase in R_0 and vice versa. Additionally, a change in the contact rate between the susceptible and infected populations induces the same percentage change in the value of R_0. For example, the simulated values evince that a 20% increase in the rate of contact between the susceptible and the infected population will induce a 20% increase in the value of the basic reproductive number, while a 20% decrease in the rate of contact between the susceptible and infected populations will induce a 20% decrease in the value of the basic reproductive number. This confirms the results in [14]. An increase in the rate of application of FPPEs (π_1) by 20% is associated with approximately 41% decrease in R_0, while a decrease in π_1 by 20% corresponds to a 41% increase in R_0. This shows that the basic reproductive number has the same degree of responsiveness to both increase and decrease in FPPEs application. The susceptible population suffers the same risk for not applying FPPEs relative to the benefit of applying FPPEs. In respect of the recovery rate (μ_2), the basic reproductive number is relatively less responsive and is negatively correlated. For instance, a 20% increase in recovery correlates with about 13.5% decrease in the basic reproductive number, whereas the same percentage decrease induces an approximately 18.4% increase in the basic reproductive number. Although the basic reproductive number is less responsive to the rate of recovery, the role of recovery in epidemiology such as COVID-19 should not be downplayed. A clear confirmation of the respective roles of rate of transmission (Figure 4), rate of contact (Figure 5), rate of FPPEs application (Figure 6), and rate of recovery (Figure 7) in the spread of COVID-19 infection has been presented (Figures 4 to 7). It is important to mention the

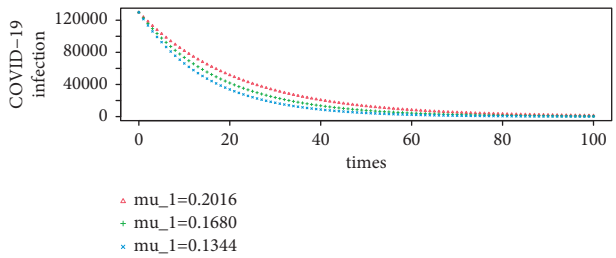

Figure 4: Simulation of COVID-19 infection at different rates of transmission. COVID-19 infection increases as the transmission rate of infection μ_1 increases from 0.1344 to 0.2016.

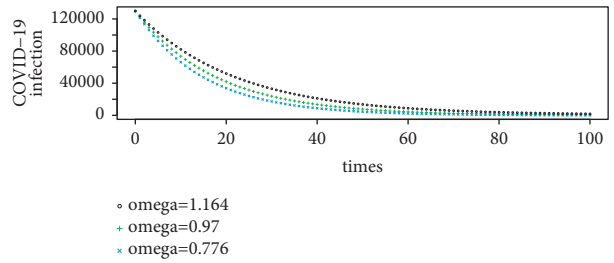

Figure 5: Simulation of COVID-19 infection at different contact rates (ω) between the susceptible and infected individuals. As ω increases from 0.776 to 1.164, there is a rightward shift in COVID-19 infection.

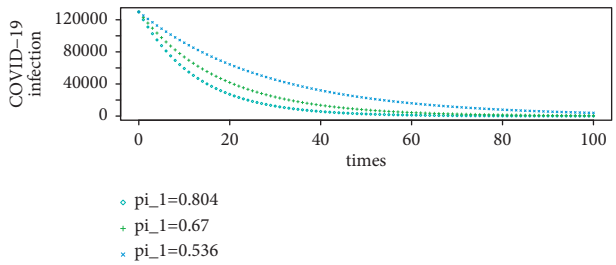

Figure 6: Simulation of COVID-19 infection at different rates (π_1) of FPPEs application. For example, π_1 increases from 0.536 to 0.67 and finally 0.804, which is indicated by a leftward shift in COVID-19 infection from the right towards the origin.

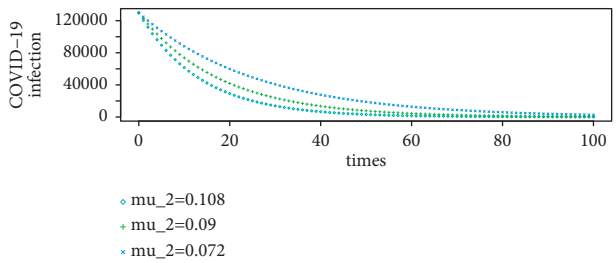

Figure 7: Simulation of COVID-19 infection at different rates (μ_2) of recovery. An increase in μ_2 from 0.072 to 0.108 is associated with an inward shift in the COVID-19 infection curve towards the origin.

negative relationship between both the natural death rate and the death rate of transmission (σ_1 and σ_2); however, efforts are needed specially to reduce the death rate of transmission through recovery. Effective treatment is, therefore, significant.

3.2. The Demand or Application of FPPEs. An essential focus of this study is to simulate the general trend of demand for fashion products, which was determined. This study categorized demand in the fashion industry into FPPEs (demand for fashion products, which is induced by the COVID-19 pandemic) and non-FPPEs (the demand for the normal fashion product prior to the emergence of the COVID-19 pandemic). Some interesting results were revealed by the outcome of the simulation.

It is significant to report a very surprising observation in connection with the relationship between the transmission rate of infection and the net demand for products of the fashion industry. The relationship was revealed to be direct.

For instance, with a 20% increase in the infectious rate of COVID-19 transmission (μ_1), the simulated value indicates an approximately 4.5% growth in the general demand for fashion products. As noted in [26], this could be explained by the effectiveness of government policies on COVID-19 precautionary and safety measures such as FPPEs application. The complimentary efforts of the susceptible population in adhering to precautionary or safety regulation should also be recommended in this regard. A reduction of the rate of infection also corresponds to an approximately 6.7% reduction in the net demand for fashion products. Possible explanations will reveal the laxity in policy stringency on precautionary and safety interventions due to the downward trend of the transmission rate of infection [30, 43], which immediately reduces the application of FPPES in the face of tight bans on social activities or events, which requires certain fashionable products (Figure 8). As experienced in the era of the acuteness or seriousness of the pandemic, government lockdown policies and individual restrictive movement interventions due to fear of being infected limited the desire to patronize general fashion products, which are occasioned for social activities. If the susceptible population perceives the infectious rate of transmission to suddenly decline, the demand for fashion products will be worsened, in the short-run, by a sudden decline in the application of FPPEs. Higher rates of infections are the results of high rate of interaction between the susceptible and the infected groups of the population, with all other things remaining constant. Clearly, the rate of contact simulates a similar pattern of variation in demand for the products of the fashion industry as does the transmission rate due to infection (Figure 9). Thus, as a result of emotional anxiety, perceived risk of infection, fear of illness or pandemic, virus anxiety, and emotional contagion [31–36], which are associated with perceived higher rates of transmission and contacts, the demand for FPPEs and its application will increase.

A variation in government policy restrictions on precautionary measures induces the same change on the general demand for fashion products. For instance, a 20% increase in policy efficiency of precautionary measures, such as the application of FPPEs, associates with an approximately 20% increase in the demand for fashion products. Similarly, a 20% downward variation in policy on precautionary measures corresponds to the same percentage decrease in the general demand for fashion products (Figure 10). On the other side of government policy restrictions centered on reducing the spread or rate of infection such as lockdown restriction and other restrictions on social activities or events, an inverse relationship can be established with the general demand for fashion products. This is the initial inverse repercussion of the outbreak of the COVID-19 pandemic on the demand for general economic products of which fashion products represent a fraction. Government restrictive policies on movements and other social events reduce the demand for usual fashion products. This inverse relationship has clearly been evidenced from the simulated outcomes of this study. An upward adjustment in lockdown policies by 20%, for example, will lead to an approximately 44% reduction in the general demand for fashion products. On the other hand, a 20% relaxation in lockdown policies induces approximately 400% growth in the general demand for fashion products (Figure 11). Clearly, the increase in demand due to an increase in the application of FPPEs is approximately 356% below the increase in demand due to relaxed movement-based restrictions or lockdown policies. Similarly, the decrease in demand due to a reduction in the application of FPPEs is also 6%, approximately above the increase in demand due to the increase in lockdown policies. Thus, the general demand for fashion products will significantly shoot up with the disappearance of COVID-19 and its associated restrictions on movement and other social events. This result indicates that restrictions on movements and other socioeconomic activities go with low demand for fashion products. This result can be linked to the findings on air purity due to lockdown in [29], since low patronage for fashion products in a pandemic could be linked to decongestion, which also, to some extent, associates with lower rate of air pollution.

The responsiveness of the general demand for fashion products to a variation in the COVID-19 recovery rate is relatively negative. As has been revealed by the simulated results, a 20% increase in the recovery rate comes with an approximately 4% reduction in the demand for fashion products, while a reduction in the COVID-19 recovery rate by 20% is associated with 4% growth in demand for fashion products (Figure 12). As more of the COVID-19 infected cases recover from infection, the tendency of handling the pandemic as a normal disease will be high; and precautionary and safety measures or interventions at the individual level will be relaxed, which may imply a reduction in the application of FPPEs, and hence, its demand in the face of very stringent antisocial events regulations. Thus, it can be confirmed, as in [31], that higher rates of recovery associate with emotional anxiety and fear, which will drive the demand for FPPEs higher. This, therefore, explains the fact that FPPEs application has a high tendency of reducing emotional anxiety driven by the fear of infection and possible death. However, if an increase in the rate of recovery from COVID-19 infections comes with a total lifting of all policies, the general demand for fashion products will significantly increase.

The impact of personal level intervention, which measures the effectiveness in the rate of FPPEs application on increasing the demand of FPPEs, cannot be downplayed. The rate of FPPEs application is a direct correlate of the general demand for the products of the fashion industry with a high degree of responsiveness. Reflecting from the outcome of the simulation, a 20% increase in the intensity of personal intervention in respect of FPPEs application (k_1) associates with about 150% increase in general demand for fashion products. This is due to an increase in the demand for FPPEs in response to policy enforcement on preventive measures and adherence of the susceptible population to the same measures as well as their own personal initiatives. Reflecting in the converse direction, a 20% reduction in k_1 associates with an approximately 38% reduction in the general demand for fashion products (Figure 13). This may be explained by

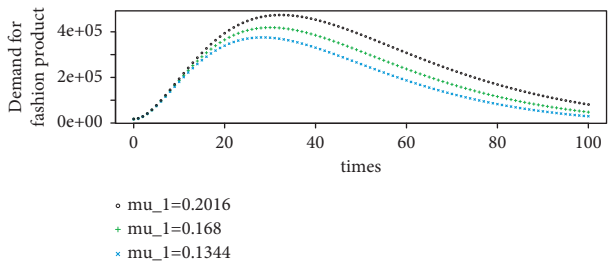

FIGURE 8: Simulation of demand for fashion products at three different rates (0.134, 0.168, and 0.2016) of μ_1. As μ_1 increases, the demand for fashion products shifts outward from the origin (left) to the right.

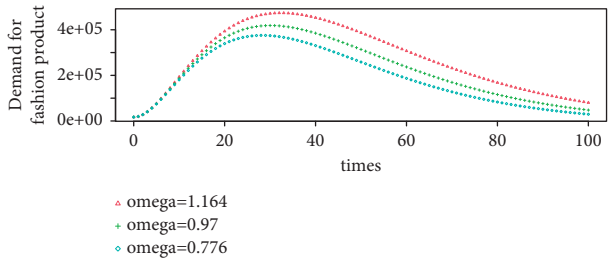

FIGURE 9: Simulation of demand for fashion products at different values of omega; $\omega = 0.776,\ 0.97$ and 1.164. As ω increases through these rates, the demand for fashion products increases.

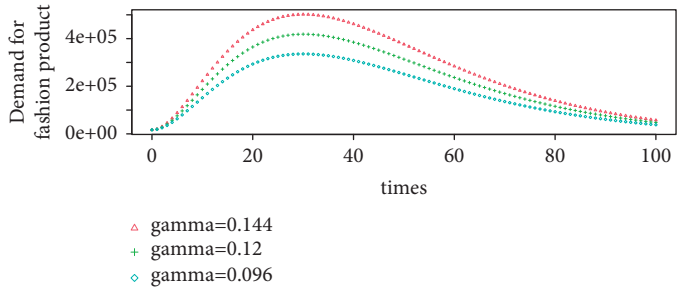

FIGURE 10: Time series simulation of the demand for fashion products at three different rates (γ) of control of safety measures to enforce the application of FPPEs. The rate of enforcing safety measures such as the application of FPPEs increases (from 0.096 to 0.144), and the demand for fashion products shifts bodily outward, indicating an increase in demand.

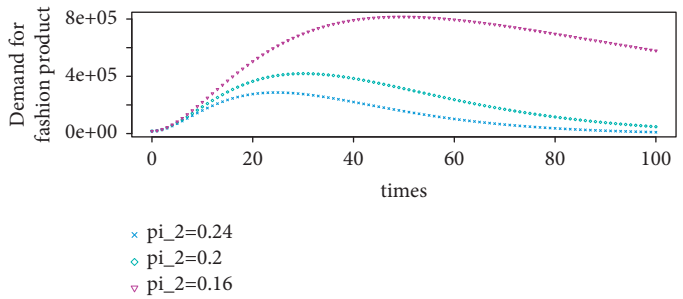

FIGURE 11: Simulation of the demand for fashion products at different rates of contact/interaction-based policy restrictions. This is aimed at decongesting the population, especially lockdowns, travelling restrictions, closure of schools, entertainment centers markets, band on social events, etc. The rate of interaction-based restriction π_2 increases from 0.16 to 0.2 and finally, to 0.24, which is associated with an inward shift in the demand curve for fashion products.

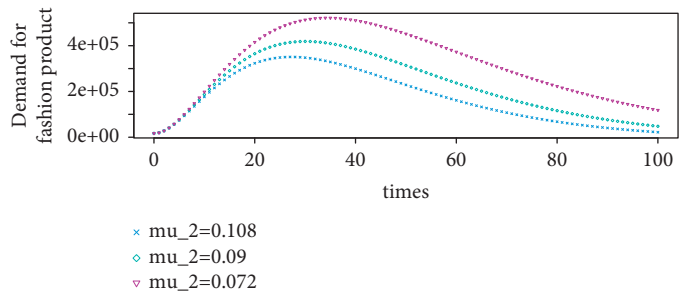

FIGURE 12: Simulation of demand for fashion products at different rates of recovery $\mu_2 = 0.072$, 0.09 and 0.108. The rate of recovery from COVID-19 μ_2 increases, while the demand for fashion products shifts inward, indicating a decline in demand.

unenforced policies and negligence of precautionary interventions by the susceptible population. It is important to reflect on the degree of responsiveness of the general demand for fashion products to increase in the effective rate of FPPEs application, which is high (in excess of 112%) compared to its degree of responsiveness to decrease in FPPEs application.

3.3. General Government Policy Regulation. The role of the government in containing the spread of COVID-19 transmission and other socioeconomic effects of COVID-19 infection is very paramount. The stringency of policies by various governments in fighting COVID-19 infection is a function of many factors such as the rate of transmission, number of infected individuals, rate of recovery, and many more. For this study, the policy stringency parameter was adopted from a study that estimated the policy stringency of governments of various countries in their quest to combat the spread of COVID-19 infection [43]. There was a stringency index of 45% around which a simulation of 20% change was considered. The magnitude of this stringency parameter depends on an infection threshold given by I_{trh} below which policy effect of the government is negative, at which level the policy effect is zero, and above which the policy effect is positive. That is, $dG/dt < 0$ if $I < I_{\text{trh}}$, $dG/dt = 0$ if $I = I_{\text{trh}}$, and $dG/dt > 0$ if $I > I_{\text{trh}}$. Considering $I = 91,954$ number of infected individuals (cumulative) as the steady state equilibrium value for I in the model at the given values of the parameters, a threshold value $I_{\text{trh}} = 1000$ will yield effective results. The value was carefully chosen to ensure positive policy effects. At a policy stringency rate of 0.45 and a relaxation force $\mu_4 = 0.1$, the effect of government policy regulation is positive. This partly provides an explanation for Ghana's remarkable performance in containing the spread of the disease. Other countries that have consistently not relaxed their stringency indices have equally achieved outstanding results as far as containing the spread of infection is concerned. The higher the value of the threshold, the better the performance of government policy regulation. For instance, increasing the threshold by 20% corresponds to a 2-percent reduction in the net government policy regulation, while a 20% reduction in disease threshold will improve the net policy performance by 2 percent. It is important to critically observe that $I_{\text{trh}} = 91,954$ implies $dG/dt = 0$, and $I_{\text{trh}} = 92,000$, similarly, implies $dG/dt < 0$. To explain further the effects of the policy threshold, an inverse relationship is also confirmed with the net demand for fashion products. For example, varying the policy threshold parameter by 20% induces a zero-point two percent (0.2%) variation on the net demand for fashion products (Figure 14). This makes the policy threshold parameter important in regulating COVID-19 FPPEs related safety measures. It is, therefore, eminent to always keep down the threshold target to promote an effective policy response.

The rate of change in government policy regulation is directly proportional, by the policy stringency index (β), to the difference between the number of infections and the disease threshold, and inversely proportional to itself by the relaxation force (μ_4). For instance, an increase in policy stringency index by 20% implies a corresponding increase in government policy regulation by 20%, while a 20% reduction in policy stringency index may induce a corresponding decrease in net government policy regulation by the same percentage decrease. On the other hand, the net government policy regulation will decrease by approximately 17% due to an increase in policy relaxation force by 20%, while a reduction in government policy relaxation force will cause an increase in total government policy regulation by 25%. The sharp change of government policy regulation in response to a reduction in policy relaxation force should be noted in comparison with its relative response to an increase in the government policy relaxation force. The effect of government policy regulation on the demand for fashion products can be confirmed since a 20% variation in the policy stringency parameter corresponds the same percentage variation in the demand for fashion products (Figure 15). Similarly, a 20% increase in the policy relaxation force induces a 17% (approximately) decrease in the net demand for fashion products, but a 20% decrease induces a 25% (approximately) in the net demand for fashion products (Figure 16).

Both the policy stringency and policy relaxation parameters should be effectively applied to maximize the effectiveness of government policies across various dimensions. This will reduce the transmission effect of infection [30, 43], which increases as a result of increased interaction between the infected and susceptible population. The spread of infection will, therefore, be flattened through increase in the application of FPPEs, which ultimately leads

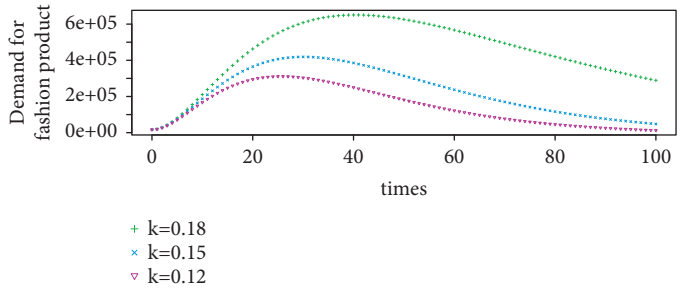

Figure 13: Simulation of the demand for fashion products at different effective rates of FPPEs application due to strict adherence to safety and precautionary measures. The effective rate of application (k) increases from 0.12 to 0.18, and the demand for fashion products shifts outward, signifying an increase in demand.

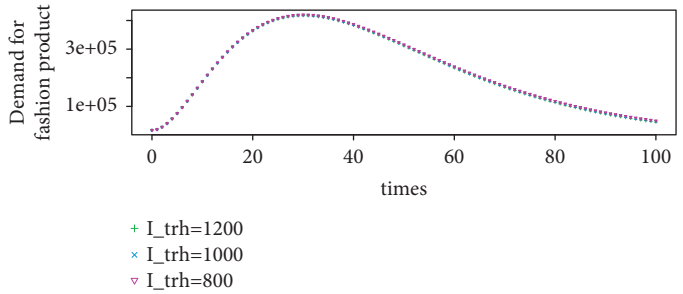

Figure 14: Simulation of the demand for fashion products at different values of the disease threshold I_{trh}. Threshold of government policy regulation declines, and the demand for fashion products increases.

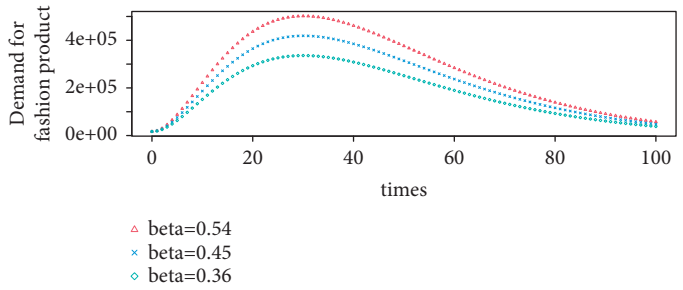

Figure 15: Simulation of the demand for fashion products at different rates of policy stringency. Policy stringency rate (β) declines from 0.45 to 0.36, and the demand shifts inward towards the horizontal axis, showing a fall. On the other hand, β increases from 0.45 to 0.54, which faces a corresponding increase in the demand for fashion products as indicated by the outward shift of the curve.

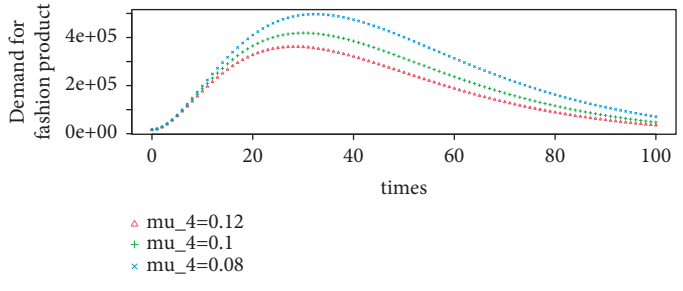

Figure 16: Time series simulation of the demand for fashion product at different rates (μ_4) of policy relaxation. As μ_4 increases from 0.08 to 0.12, the demand for fashion products decreases. The curve shifts inward as μ_4 increases.

to a high demand for FPPEs. Although lockdown and other restrictive policies are inverse correlates of the general demand for fashion products, policy effectiveness on the application of FPPEs in addition to individual interventional efforts will recompense such a fall in demand, while the disease is still vibrant.

4. Conclusions

The study was a complete simulation of the effect of COVID-19 pandemic on the growth of the demand for fashion products, and the role of the demand for FPPEs in curtailing the spread of COVID-19 transmission. The study covered model formulation, qualitative analysis, computation of basic reproductive number, assessing stability of the model, simulation, and discussion of results. Based on the results, the following discoveries were noted:

The variables proved to be positive and bounded within the region $\Phi = \{(S, I, R, A, G) \in R^5: S + +I + R \leq \pi_s N / \sigma_1, A \leq K/k_2, G \leq \beta I/\mu_4\}$. The disease-free equilibrium was both locally and globally asymptotically stable for values of the basic reproductive number less than unity ($R_0 \leq 1$), whereas the disease endemic equilibrium is also locally and globally asymptotically stable for $R_0 \geq 1$. The natural death rate, the death rate of transmission, the rate of application of FPPEs, and the recovery rates were inverse correlates of the basic reproductive number, while the transmission rate of infection and the rate of contact between infected and susceptible individuals were positive correlates of the basic reproductive number. The intensity of control on safety measures increased the demand for fashion products. Furthermore, effective application of FPPEs (personal intervention in respect of FPPEs application), the transmission rate of infection, the rate of contact, and policy stringency were positive correlates of the demand for products of the fashion industry. On the other hand, government restrictions on movement, policy relaxation force, recovery rates, and disease threshold were inverse correlates of the demand for fashion products. Thus, COVID-19 played a double-edged role in increasing the demand for products of the fashion industry through the application of FPPEs on the one hand, while, on the other hand, it played the role of decreasing the demand for the products of the fashion industry through restrictions on various social events. However, the results suggest that the declining effect outweighs the increasing effects resulting in a negative net effect. Giving the inverse relationship between the rate of application of FPPEs (or the demand for fashion products) and the basic reproductive number R_0, the demand for fashion products played a significant role in reducing the spread of COVID-19 infection. All other positive correlates of the demand for FPPEs such as the government policy stringency were significant in decreasing the rate of infection of COVID-19. Other COVID-19 declining factors included effective application of FPPEs and restriction on safety measures. Thus, the demand for FPPEs and its application had the tendency to reduce emotional anxiety (fear of the virus or pandemic) and perceived risk of infection. As the results of the sensitivity analysis suggested, governments should prioritize policy interventions in support of FPPEs application to complement all recommended PPEs.

Overall, the persistence of COVID-19 infection had the tendency to increase the demand for fashion products if individual safety interventions through strict adherence were enough to supplement government restrictions on this safety measures. Recovery in the event of lockdowns and other interaction-based restrictions may significantly reduce the demand for fashion products. Despite that, the demand for fashion products will increase significantly in a pandemic-free environment.

The study was not without limitations, one of which was the sketchy or nearly nonexisting literature on the impact of COVID-19 on demand for fashion products. In addition, most of the parameters were based on simulations, which made it difficult to validate the model with real data; however; simulation has proven to be significant in providing useful results that conforms to reality. Thus, the simulated results entail relevant health and economic implications for all stakeholders. Considering the global impact of COVID-19, it becomes imperative to apply a wholistic intervention to ensure that this pandemic is completely wiped out. It is recommended that FPPEs be used together with other nonpharmaceutical interventions. Operators in the fashion industry must also be dynamic enough to adjust to the new trend of taste for fashion products. Since the result suggests that a faster rate of decline in government policy restriction in line with the application of FPPES is associated with a slower declining rate of COVID-19 infection, a small negligence may trigger a resurgence of infection at a devastating rate. Government should, therefore, be consistent in maintaining high policy stringency. It is a candid suggestion to all citizens to continuously observe all COVID-19 safety or precautionary protocols until the disease goes into total extinction.

We recommend that future research in this area should consider the effect of government policy stringency in the light of vaccination on both the demand and supply of fashion-based PPEs in an susceptible-exposed-infected-recovery-susceptible (SEIRS) model.

Data Availability

Data are available upon request to the corresponding author.

Conflicts of Interest

The authors declare that they have no conflicts of interest.

Authors' Contributions

All authors conceptualized the idea and prepared the framework of the manuscript. John Awuah Addor developed the ODEs and performed the qualitative analysis. Anthony Joe Turkson performed the simulations and prepared the manuscript according to the guidelines of the journal. Douglas Yenwon Kparib developed and tested some of the equations and assisted in executing the simulations. All authors did the final editing of the work and read it thoroughly before the final submission.

References

[1] L. A. Asante and R. O. Mills, "Exploring the socio-economic impact of covid-19 pandemic in market places in Urban Ghana," *Africa Spectrum*, vol. 55, 2020.

[2] J. Y. T. Mugisha, J. Ssebuliba, J. N. Nakakawa, C. R. Kikawa, and A. SsematimbaI, "Mathematical Modeling of COVID-19 Transmission Dynamics in Uganda: Implications of Complacency and Early Easing of Lockdown," *PLoS One*, vol. 16, 2021.

[3] WHO, "Emergencies diseases novel cornavirus-2019," 2020, http://who.int/emergencies/diseases/novel-coronavirus-2019/available online.

[4] H. Shi, X. Han, N. Jiang, Y. Cao, O. Alwalid, and J. Gu, "Radiological findings from 81 patients with COVID19 pneumonia in Wuhan, China: a descriptive study," *The Lancet Infectious Diseases*, vol. 20, no. 4, pp. 425–34, 2021.

[5] Q. Li, X. Guan, P. Wu et al., "Early transmission dynamics in wuhan, China, of novel coronavirus-infected pneumonia," *New England Journal of Medicine*, vol. 382, no. 13, pp. 1199–1207, 2020.

[6] P. Wu, X. Hao, E. H. Y. Lau et al., "Real-time tentative assessment of the epidemiological characteristics of novel coronavirus infections in Wuhan, China, as at 22 January 2020," *Euro Surveillance*, vol. 25, no. 3, Article ID 2000044, 2020.

[7] J. T. Wu, K. Leung, and G. M. Leung, "Nowcasting and forecasting the potential domestic and international spread of the 2019-nCoV outbreak originating in Wuhan, China: a modelling study," *The Lancet*, vol. 395, pp. 689–697, Article ID 10225, 2020.

[8] L. Lin, G. Yang, L. Yang, and D. He, "The association between domestic train transportation and novel coronavirus (2019-nCoV) outbreak in China from 2019 to 2020: a data-driven correlational report," *Travel Medicine and Infectious Disease*, vol. 33, Article ID 101568, 2020.

[9] WHO, "World health organization coronavirus disease (COVID-2019), situation reports," 2020, https://www.who.int/emergencies/diseases/novel- coronavirus-2019/situation-reports/.

[10] WHO, "World Health organization, coronavirus disease (COVID-19) dashboard," 2020, https://covid19.who.int/.

[11] CDC, "For Disease Control and Prevention, Coronavirus Disease (COVID-19)," 2020, https://www.cdc.gov/coronavirus/2019-nCoV/index. Html.

[12] H. Nishiura, N. M. Linton, and A. R. Akhmetzhanov, *Journal of Clinical Medicine*, vol. 9, no. 488, p. 2020.

[13] S. Zhao, S. S. Musa, T. J. Hebert et al., vol. 8, p. 8601, 2020.

[14] S. S. Musa, S. Zhao, D. Gao, Q. Lin, G. Chowell, and D. He, "Mechanistic modelling of the large-scale Lassa fever epidemics in Nigeria from 2016 to 2019," *Journal of Theoretical Biology*, vol. 493, Article ID 110209, 2020 pages.

[15] S. S. Musa, S. Qureshi, S. Zhao, A. Yusuf, U. T. Mustapha, and D. He, "Mathematical Modeling of COVID-19 Epidemic with Effect of Awareness Programs," *Infect Dis Model*, vol. 6, 2021.

[16] S. Zhao, L. Stone, D. Gao et al., "Imitation dynamics in the mitigation of the novel coronavirus disease (COVID-19) outbreak in Wuhan, China from 2019 to 2020," *Annals of Translational Medicine*, vol. 8, no. 7, 2020.

[17] E. Kenu, A. Magdalene, K. L. Malm et al., "Epidemiology of COVID-19 outbreak in Ghana," *Koram5 Ghana Med J*, vol. 54, no. 4, pp. 5–15, 2020.

[18] M. Gilbert, G. Pullano, F. Pinotti et al., "Preparedness and vulnerability of African countries against importations of COVID-19: a modelling study," *The Lancet*, vol. 395, pp. 871–877, Article ID 10227, 2020.

[19] E. A. Iboi, C. N. Ngonghala, and A. B. Gumel, "Will an imperfect vaccine curtail the COVID-19 pandemic in the U.S.?" *Infectious Disease Modelling*, vol. 5, pp. 510–524, 2020.

[20] H. Tian, "An investigation of transmission control measures during the first 50 days of the COVID19 epidemic in China," *Science*, vol. 368, no. 6491, pp. 638–642, 2020.

[21] D. K. Chu et al., "Physical distancing, face masks, and eye protection to prevent person- to-person transmission of SARS-CoV-2 and COVID-19: a systematic review and meta-analysis," *The Lancet*, vol. 6, 2020.

[22] E. Mathieu, H. Ritchie, and E. Ortiz-Ospina, "A global dataset of COVID-19 vaccinations," *Nat Hum Behav*, vol. 5, 2021.

[23] N. M. Ferguson, *Impact of Non-pharmaceutical Interventions (NPIs) to Reduce CoViD-19 Mortality and Healthcare Demand*, Imperial College CoViD-19 Response Team, UK, 2020.

[24] B. Tang, X. Wang, Q. Li et al., "Estimation of the transmission risk of the 2019-nCoV and its implication for public health interventions," *Journal of Clinical Medicine*, vol. 9, no. 2, p. 462, 2020.

[25] C. N. Ngonghala, E. Iboi, S. Eikenberry et al., "Mathematical assessment of the impact of non-pharmaceutical interventions on curtailing the 2019 novel Coronavirus," *Mathematical Biosciences*, vol. 325, Article ID 108364, 2020.

[26] Q. Lin, S. Zhao, D. Gao et al., "A conceptual model for the coronavirus disease 2019 (COVID-19) outbreak in Wuhan, China with individual reaction and governmental action," *International Journal of Infectious Diseases*, vol. 93, pp. 211–216, 2020.

[27] Z. Memon, S. Qureshi, and B. R. Memon, *Assessing the Role of Quarantine and Isolation as Control Strategies for COVID-19 Outbreak: A Case Study*, Solitons & Fractals, Chaos, 2021.

[28] S. E. Eikenberry, M. Mancuso, E. Iboi et al., "To mask or not to mask: modeling the potential for face mask use by the general public to curtail the COVID-19 pandemic," *Infectious Disease Modelling*, vol. 5, pp. 293–308, 2020.

[29] K. Shehzad, F. Bilgili, E. Koçak, L. Xiaoxing, and M. Ahmad, "COVID-19 outbreak, lockdown, and air quality: fresh insights from New York City," *Environmental Science and Pollution Research*, pp. 1–13, 2021.

[30] F. Bilgili, M. Dundar, S. Kuşkaya et al., "The age structure, stringency policy, income, and spread of coronavirus disease 2019: evidence from 209 countries," *Frontiers in Psychology*, vol. 4042, 2021.

[31] S. Cohen and E. Nica, "COVID-19 pandemic-related emotional anxiety, perceived risk of infection, and acute depression among primary care providers," *Psychosociological Issues in Human Resource Management*, vol. 9, no. 2, pp. 7–20, 2021.

[32] D. Adams and M. Grupac, "Stress-related psychiatric disorders, clinically significant depression, and elevated anxiety symptoms among medical personnel providing care to COVID-19 patients," *Psychosociological Issues in Human Resource Management*, vol. 9, no. 2, pp. 133–146, 2021.

[33] K. Wade and K. Valaskova, "Acute depression, moral dilemmas, and illness fears in COVID-19 frontline healthcare providers," *Psychosociological Issues in Human Resource Management*, vol. 9, no. 2, pp. 91–104, 2021.

[34] G. Lăzăroiu and C. Adams, "Viral panic and contagious fear in scary times: the proliferation of COVID-19 misinformation and fake news," *Analysis and Metaphysics*, vol. 19, pp. 80–86, 2020.

[35] E. Dobson-Lohman and A. M. Potcovaru, "Fake news content shaping the COVID-19 pandemic fear: virus anxiety, emotional contagion, and responsible media reporting," *Analysis and Metaphysics*, vol. 19, pp. 94–100, 2020.

[36] S. Bratu, "The fake news sociology of COVID-19 pandemic fear: dangerously inaccurate beliefs, emotional contagion, and

conspiracy ideation," *Linguistic and Philosophical Investigations*, no. 19, pp. 128–134, 2020.

[37] C. C. Chavez, S. Blower, P. Van den Driessche, D. Kirschner, and A. A. Yakubu, *Mathematical Approaches for Emerging and Reemerging Infectious Diseases*, Springer science and Business Media, Berlin/Heidelberg, Germany, 2002.

[38] K. P. Vatcheva, J. Sifuentes, T. Oraby, J. C. Maldonado, T. Huber, and M. C. Villalobos, "Social distancing amd testing as optimal strategies against the spread of COVID-19 in the Ri0o grande valley of Texas," *Infectious disease modelling*, vol. 6, pp. 729–742, 2021.

[39] D. Dwomoh, S. Iddi, B. Adu et al., "Mathematical modeling of COVID-19 infection dynamics in Ghana: impact evaluation of integrated government and individual level interventions," *Infectious Disease Modelling*, vol. 6, pp. 381–397, 2021.

[40] Ghana-2022, "World Bank Statistics," 2021, https://www.macrotrends.net/countries/GHA/ghana/...deathrate.

[41] L. Chen, J. Xiong, L. Bao, and Y. Shi, "Convalescent plasma as a potential therapy for COVID-19," *The Lancet Infectious Diseases*, vol. 20, no. 4, pp. 398–400, 2020.

[42] D. Serwaa, E. Lamptey, A. B. Appiah, E. Kumi Senkyire, and J. K. Ameyaw, "Knowledge, risk perception and preparedness towards corona virus disease-2019 (COVID-19) outbreak among Ghanaians, quick online cross-sectional study," *Pan African Medical Journal*, vol. 35, no. 2, 2020.

[43] T. Hale, A. Petherick, T. Philips, and S. Webster, *Variation in Government Responses to COVID-19. Working Paper*, Blavatnik School of Government, University of Oxford, Oxford, UK, 2020.